

HEAT AND MASS TRANSFER DURING VAPOR ABSORPTION BY A STAGNANT SOLUTION LAYER

V. E. Nakoryakov, N. S. Bufetov, N. I. Grigor'eva, and R. A. Dekhtyar'

UDC 536.423.4

Based on simple models of nonisothermal absorption for the cases of long and short times, the effect of the heat-generation and heat-extraction rates on vapor absorption by a stagnant solution layer is analyzed. Models taking into account and ignoring the motion of the interface between the phases are considered. Results of an experimental study of steam absorption by a stagnant water/LiBr solution are described. Time dependences of temperatures at various heights inside the liquid layer and of the absorbed mass, and also temperature and concentration profiles at various times, are reported. A comparison of predicted values with experimental data is given.

Key words: *absorption, heat and mass transfer, diffusion, solution, concentration, temperature.*

Introduction. Absorption of steam by salt solutions accompanied by intense heat generation is widely used in heat pumps and absorption refrigerators. Most frequently, absorption proceeds on solution film flows down surfaces through which the heat released during the absorption is extracted. For this reason, most of works treated the case of film absorption. For instance, based on simple models of nonisothermal film absorption, exact analytical solutions were derived [1–4], including self-similar solutions [2, 4]; numerical data were presented in [5–9]. Experimental studies of film absorption were reported and a comparison between numerical and experimental data was given in [10, 11].

The present-day requirements to high-performance technical apparatus necessitate further search for new methods of intensification of transfer processes in absorbers. One of such methods employs surfactants introduced to solutions and giving rise to small-scale surface convection, which intensifies heat and mass transfer. However, it is extremely difficult to discriminate between the contributions to heat and mass transfer due to the main flow and due to convection caused by the surface-tension gradient in experiments aimed at revealing the effect of surfactants on film absorption. In this case, it is of interest to study vapor absorption by a stagnant solution layer without any forced flow [12]. The theoretical and experimental data on local heat- and mass-transfer characteristics in absorption without surfactants can be used as reference data to be compared with similar results obtained with surfactants added to solutions. In [12], such a comparison was made only for one integral characteristic (variation of the absorbed mass in time). A study of vapor absorption by a stagnant solution layer is also of interest in view of the fact that, in this case, it is possible to take into account the contributions due to individual factors affecting heat and mass transfer, such as generation of heat, motion of the interface, heat removal through the wall, and surfactants present in the solution. With all these factors except for the effect due to surfactants and under some additional assumptions, it is possible to derive simple analytical solutions [13, 14], which can be conveniently analyzed and compared with experimental data. In addition, in the case of vapor absorption by a stagnant liquid layer, it is possible to more adequately reproduce experimental conditions close to those assumed in theoretical models.

Model of Nonisothermal Absorption. The problem about heat and mass transfer in a binary solution is considered under the following assumptions which, in particular, are valid for systems used in absorption heat pumps and refrigerators. During the whole process, the density of the solution, thermophysical parameters, and

Kutateladze Institute of Thermal Physics, Siberian Division, Russian Academy of Sciences, Novosibirsk 630090. Translated from *Prikladnaya Mekhanika i Tekhnicheskaya Fizika*, Vol. 44, No. 2, pp. 101–108, March–April, 2003. Original article submitted September 18, 2002.

transfer coefficients remain constant. During the absorption, the vapor pressure remains unchanged. The absorption heat is released at the interface to be spent only on heating of the liquid phase (solution). The bottom-surface temperature T_w is maintained constant and, in the general case, can differ from the initial temperature of the solution T_0 . The solution is composed of two components, one being absorbed from the gas phase bordering on the solution, and the other being neither consumed nor added to the solution. Thus, the interface is impermeable for the second component and moves with a certain velocity $V(t)$.

The vapor–solution two-phase system at the interface is in an equilibrium state described, for a binary solution under constant pressure, by the temperature dependence of the absorbed substance concentration $C = f(T)$. In sufficiently narrow concentration and temperature intervals, this dependence can be approximated by the linear function $C_i = k_1 - k_2 T_i$, where k_1 and k_2 are pressure-dependent coefficients.

The heat released during the absorption causes time variation of the equilibrium temperature at the interface and, as a consequence, time variation of the concentrations according to the conditions of equilibrium. Thus, the point with the coordinates (C_i, T_i) travels along the equilibrium curve. At each time, including the initial one, the exact position of this point is unknown beforehand.

According to the assumptions stated above, heat and mass transfer in the solution layer obeys the equations of energy and mass conservation, which can be conveniently written in the coordinate system attached to the moving interface:

$$\frac{\partial T}{\partial t} + V \frac{\partial T}{\partial x} = a \frac{\partial^2 T}{\partial x^2}, \quad \frac{\partial C}{\partial t} + V \frac{\partial C}{\partial x} = D \frac{\partial^2 C}{\partial x^2}.$$

The initial conditions are

$$t = 0: \quad T = T_0, \quad C = C_0;$$

the condition at the interface between the phases are

$$x = 0: \quad C_i = f(T_i), \quad -\lambda \frac{\partial T}{\partial x} = r_a m_a; \quad (1)$$

the boundary conditions at the bottom surface are

$$x = \delta(t): \quad T = T_w, \quad \frac{\partial C}{\partial x} = 0.$$

Here $V(t) = -(D/(1 - C_i))\partial C/\partial x$ ($x = 0$) is the velocity of the interface determined by the condition of interface impermeability for the second component $m_b = (1 - C_i)\rho V - \rho D\partial(1 - C)/\partial x = 0$, m_a is the density of the mass flux of the absorbed substance,

$$m_a = C_i \rho V - \rho D \frac{\partial C}{\partial x} = -\frac{\rho D}{1 - C_i} \frac{\partial C}{\partial x},$$

t is the time, δ is the thickness of the liquid layer, a is the thermal diffusivity, D is the diffusivity, λ is the thermal conductivity, ρ is the density of the solution, and r_a is the absorption heat.

Solution over Short Times. In [13, 14], absorption is considered over the time interval during which heat removal through the bottom does not affect the temperature variations near the interface, i.e., during which the thermal boundary layer propagating, as it forms, from the interface has not yet met the thermal boundary layer on the rigid wall (bottom surface). In addition, systems are considered for which the Lewis number $Le = D/a$ is much smaller than unity, i.e., for which the thickness of the diffusion boundary layer is small (much smaller than the thickness of the thermal boundary layer). Thus, either the case of short times or the case of sufficiently thick liquid layers is treated. In this situation, the system of governing equations and the boundary conditions can be written in dimensionless form, in terms of the self-similar variable $\xi = x/(2\sqrt{at})$:

$$\frac{d^2 \theta}{d\xi^2} + 2\left(\xi + \frac{\sqrt{LeDt}}{1 - C_i} \frac{\partial C}{\partial x} \Big|_{x=0}\right) \frac{d\theta}{d\xi} = 0, \quad Le \frac{d^2 \gamma}{d\xi^2} + 2\left(\xi + \frac{\sqrt{LeDt}}{1 - C_i} \frac{\partial C}{\partial x} \Big|_{x=0}\right) \frac{d\gamma}{d\xi} = 0,$$

$$\xi \rightarrow \infty: \quad \theta = 0, \quad \gamma = 0;$$

$$\xi = 0: \quad \gamma_i = F(\theta_i); \quad (2)$$

$$\frac{d\theta}{d\xi} = KLe \frac{C_e - C_0}{1 - \gamma_i(C_e - C_0) - C_0} \frac{d\gamma}{d\xi}. \quad (3)$$

Here $\theta = (T - T_0)/(T_e - T_0)$, $K = r_a/[C_p(T_e - T_0)]$, $Le = D/a$, $\gamma = (C - C_0)/(C_e - C_0)$, C_e is the equilibrium concentration at the initial temperature [$C_e = f(T_0)$], T_e is the equilibrium temperature corresponding to the initial concentration [$C_0 = f(T_e)$], and C_p is the specific heat capacity.

The temperature and concentration fields acquire the form

$$\theta = \frac{\theta_i[1 - \operatorname{erf}(\xi + B)]}{1 - \operatorname{erf}(B)}, \quad \gamma = \frac{\gamma_i[1 - \operatorname{erf}((\xi + B)/\sqrt{Le})]}{1 - \operatorname{erf}(B/\sqrt{Le})}, \quad (4)$$

where $B = (\sqrt{LeDt}/(1 - C_i)) \partial C/\partial x|_{x=0}$. The constants γ_i , θ_i , and B , independent of t , are defined by system (2)–(4).

If we approximate the equilibrium condition by the linear function $C_i = k_1 - k_2 T_i$ having the slope $k_2 = (C_e - C_0)/(T_e - T_0)$, then relation (2) becomes $\theta_i + \gamma_i = 1$ and the constant B can be found from the equation

$$B = -\frac{\sqrt{Le}(C_e - C_0)\gamma_i \exp(-B^2/Le)}{\sqrt{\pi}[1 - \gamma_i(C_e - C_0) - C_0][1 - \operatorname{erf}(B/\sqrt{Le})]},$$

in which the dimensionless concentration at the interface can also be expressed in terms of the constant B :

$$\gamma_i = 1 + KB(1 - \operatorname{erf}(B))\sqrt{\pi} \exp(B^2).$$

Thus, the value of B can easily be determined in an iterative manner.

The mass-flux density at the free surface of the liquid layer is given by the formula

$$m_a = \frac{\rho\sqrt{D}(C_e - C_0)}{\sqrt{\pi t}} \frac{\gamma_i}{1 - \gamma_i(C_e - C_0) - C_0} \frac{\exp(-B^2/Le)}{1 - \operatorname{erf}(B/\sqrt{Le})}. \quad (5)$$

A comparison of (5) with an analogous formula for isothermal absorption [14] shows that heat generation and interface motion are allowed for by the last two multipliers.

Absorption with Heat Removal in the Case of Long Times. If the bottom-surface temperature T_w is maintained unchanged (lower than or equal to the temperature of the initial solution T_0), then the effect due to the cool wall gradually extends to the interface and the temperature profile becomes almost linear. Such a problem without allowance for interface motion was considered in [14]. In the present study, interface motion is ignored in the diffusion equation, and the convective component of the mass flux in the boundary condition (1) is retained. In this case,

$$\begin{aligned} \theta &= \theta_i - (\theta_0 + \theta_i)\eta, \\ \eta &= \frac{x}{\delta}, \quad \theta_0 = \frac{T_0 - T_w}{T_e - T_0}, \quad \frac{\partial \gamma}{\partial \tau} = Le \frac{\partial^2 \gamma}{\partial \eta^2}, \quad \tau = \frac{at}{\delta^2}. \end{aligned} \quad (6)$$

Here the time is measured from the moment τ_0 , at which the temperature profile can be regarded as linear.

The unknown temperature and concentration at the interface are related by the equilibrium condition and by the heat-balance condition:

$$\eta = 0, \quad \gamma = \gamma_i(\tau), \quad \theta = \theta_i(\tau), \quad \theta_i + \gamma_i = 1,$$

$$\frac{\partial \theta}{\partial \eta} = \frac{KLe(C_e - C_0)}{1 - \gamma_i(C_e - C_0) - C_0} \frac{\partial \gamma}{\partial \eta}.$$

If γ_i slowly decreases with time from an initial value γ_{i0} (dimensionless concentration at the interface at short times), then, for estimates, we can use the solution obtained in [14] for the conditions without interface motion. Then, we have

$$\gamma_i = 1 + \theta_0 - (1 - \gamma_{i0} + \theta_0) \exp(p\tau)(1 - \operatorname{erf}(\sqrt{p\tau})), \quad \theta_i = 1 - \gamma_i, \quad (7)$$

where $p = [1 - \gamma_{i0}(C_e - C_0) - C_0]^2/[K^2Le(C_e - C_0)^2]$, and we can use the value of γ_i obtained at some time step as γ_{i0} for the next time step.

For the density of the mass flux through the free surface of the liquid layer, the following simple formula results:

$$m_a = -\frac{\rho D}{1 - C_i} \frac{\partial C}{\partial x} \Big|_{x=0} = \frac{\rho D}{\delta K Le} (1 - \gamma_{i0} + \theta_0) \exp(p\tau)(1 - \operatorname{erf}(\sqrt{p\tau})).$$

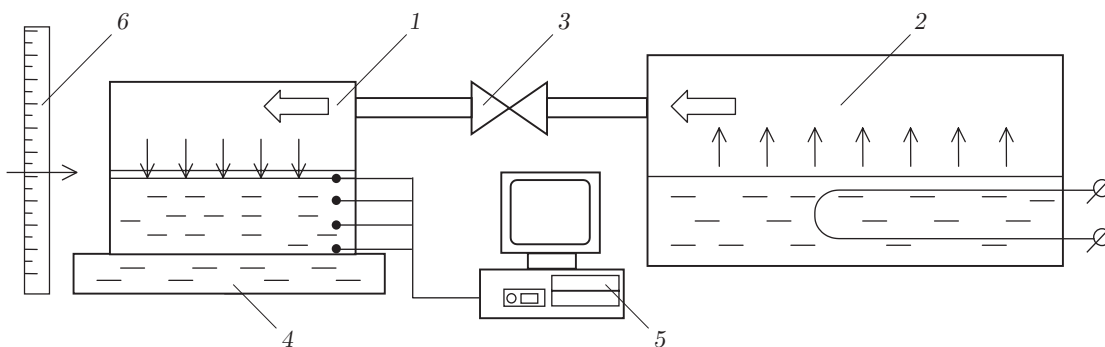


Fig. 1. Diagram of the experimental setup: 1) absorber; 2) steam generator; 3) valve; 4) water thermostat; 5) computer; 6) cathetometer.

The above analytical relations for short and long times can be used in estimating the effects due to heat-generation and heat-extraction rates on the absorption intensity, in analyzing experimental data, and in testing numerical simulations and comparing their results with experimental data obtained under more complex conditions such as, for instance, those obtained for solutions with surfactants.

Experimental Setup. The experimental study was performed on a setup consisting of an absorber and a steam generator connected by a pipeline equipped with a fast-response valve. The diagram of the setup is shown in Fig. 1.

We used an aqueous solution of lithium bromide (LiBr) as an absorbent and steam as a gas absorbate. This system is commonly used in absorption heat pumps and refrigerators. Its thermophysical and other properties are well studied and described in [15].

The absorber was a 165-mm cylindrical container 87 mm high, made of stainless steel, with a side window for visual observations and measurements of the liquid-layer thickness. The sidewalls of the absorber were 1.5 mm thick, and the bottom was 6 mm thick. Five thermocouples in protective housing in the form of capillary tubes 1 mm in diameter were introduced into the absorbent layer through the sidewalls; they were installed with an angular step of 36° in the horizontal plane and with a step of 5 mm over the height of the liquid layer. The length of the horizontal part of the thermocouples inside the container was 65 mm. The lower capillary was mounted in the immediate vicinity of the bottom, and the upper capillary at a height of 20 mm.

The thermocouples were prepared from copper and constantan wires 0.16 and 0.1 mm in diameter, respectively. Each thermocouple was calibrated so that to permit temperature measurements with accuracy better than 0.1°C . In the case of stepwise temperature variation, the indications of the thermocouples attained their steady-state values in a time shorter than 3 sec.

The heat flux through the bottom of the absorber was calculated from the readings of differential thermocouples whose junctions were located at a distance of 0.5 and 5 mm from the bottom surface. To measure the solution-concentration distribution over the height, solution samples were taken from various heights of the layer. The samplers were dead-end tubes 2 mm in diameter and had 0.8-mm holes drilled in their side surfaces. The samplers were positioned so that to allow solution sampling from desired heights, the sampling holes facing upward. This location of the tubes ensured the weakest possible mixing of the lower layers during layer-by-layer drainage of the solution.

The steam generator was a vessel whose volume was about 20 liters. Heaters for evaporating water from the LiBr solution were installed at the bottom of the vessel. Computer-controlled power supply allowed the pressure in the system to be maintained unchanged within ± 5 Pa (the pressure was monitored by a “Metran”-type pressure gauge). This allowed us to use the steam generator as a barostat.

Experimental Procedure. A concentrated solution of LiBr (0.855 ± 0.025 kg) was poured into the absorber so that to cover the protective housing of the upper thermocouple by a liquid layer of thickness 0.2–0.5 mm. Prior to an experiment, the absorber was covered with a special hood made of polyethylene film, and the temperature inside the hood was maintained unchanged with the help of a computer-controlled ohmic heater with a fan and a temperature gauge. Long-time thermostating (over periods no shorter than 12 hours) ensured a constant temperature in the liquid layer and the absence of any convective flows in the liquid before the tests. The bottom-surface temperature was maintained unchanged by cool water delivered from the water thermostat (Fig. 1).

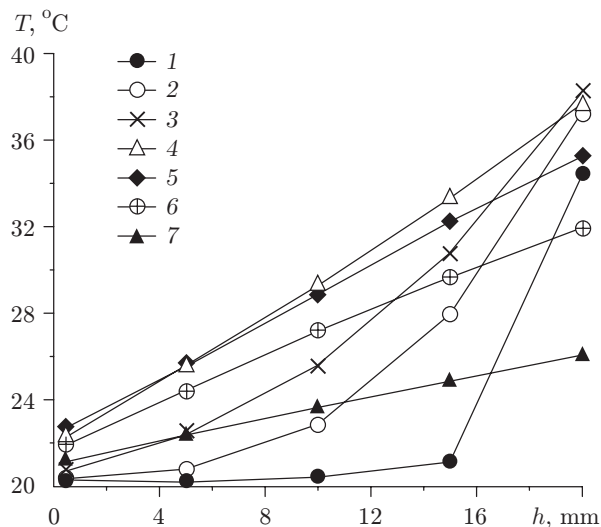


Fig. 2

Fig. 2. Temperature profiles at various times: $t = 27$ (1), 202 (2), 409 (3), 1490 (4), 4020 (5), 9910 (6), and 56,265 sec (7).

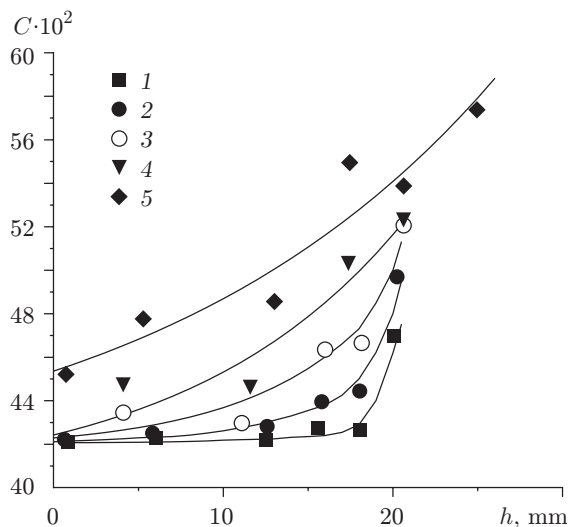


Fig. 3

Fig. 3. Concentration profiles at various times: $t = 980$ (1), 3670 (2), 7465 (3), 18,230 (4), and 56,250 sec (5).

To remove nonabsorbable impurities accumulated owing to desorption from metal, rubber, and other surfaces of the absorber and steam generator, the inner volume of the setup was evacuated through a capillary tube of diameter $d = 1$ mm during the whole test.

After the pipeline valve was open, the steam produced by the steam generator entered the absorber. Usually, the absorber and steam-generator pressures became identical after a period of 0.8 sec.

During the experiment, we checked the heat balance with allowance for the heat released during the absorption, the heat spent on solution heating, and the heat extracted through the bottom. Over a period of seven hours, the balance was found to hold rather precisely; over longer times, the decrease in the temperature difference at the bottom wall to values comparable with the measurement accuracy and the neglect of heat withdrawn through the side wall violated the balance.

In the experiments, we measured the distribution of temperature over the height of the liquid layer, the temperature difference at the absorber bottom, and the pressure in the absorber. The data were fed into a computer (Fig. 1). The thickness of the liquid layer was measured by the cathetometer within 0.01 mm.

Each experiment was terminated by closing the valve, after which the gas pumping was switched off, and atmospheric air was let in into the system. Afterwards, layer-by-layer drainage of the solution was conducted to determine the mean density and temperature of each sampled portion of the solution and the same parameters of the solution as a whole. To do this, the functional dependence of concentration on density and temperature was used [15].

To gain data on time variation of concentration, ten tests differing only in their durations (from 15 min to 15.5 h) were performed.

Experimental Results. The thermophysical properties of the solution and the experimental conditions were $a = 1.3 \cdot 10^{-7}$ m²/sec, $D = 1.27 \cdot 10^{-9}$ m²/sec, $C_p = 1980$ J/(kg·°C), $\mu = 6.94 \cdot 10^{-3}$ kg/(m·sec), $\lambda = 0.415$ W/(m·°C), $\rho = 1680$ kg/m³, $r_a = 2.725 \cdot 10^6$ J/kg, $P = 1970$ Pa, $T_0 = 20.4^\circ\text{C}$, and $C_0 = 0.42$.

Figure 2 shows the temperature profiles measured at various times. The temperature near the free surface is seen to vary only little in time for $t < 800$ sec, in line with the theoretical predictions that the equilibrium temperature at the interface and, hence, the concentration are expected to remain constant at short times. The exact value of the surface temperature was not measured, since the upper thermocouple was located 20 mm above the bottom and the thickness of the liquid layer increased with time. At long times, the temperature profiles became linear, and the surface temperature decreased.

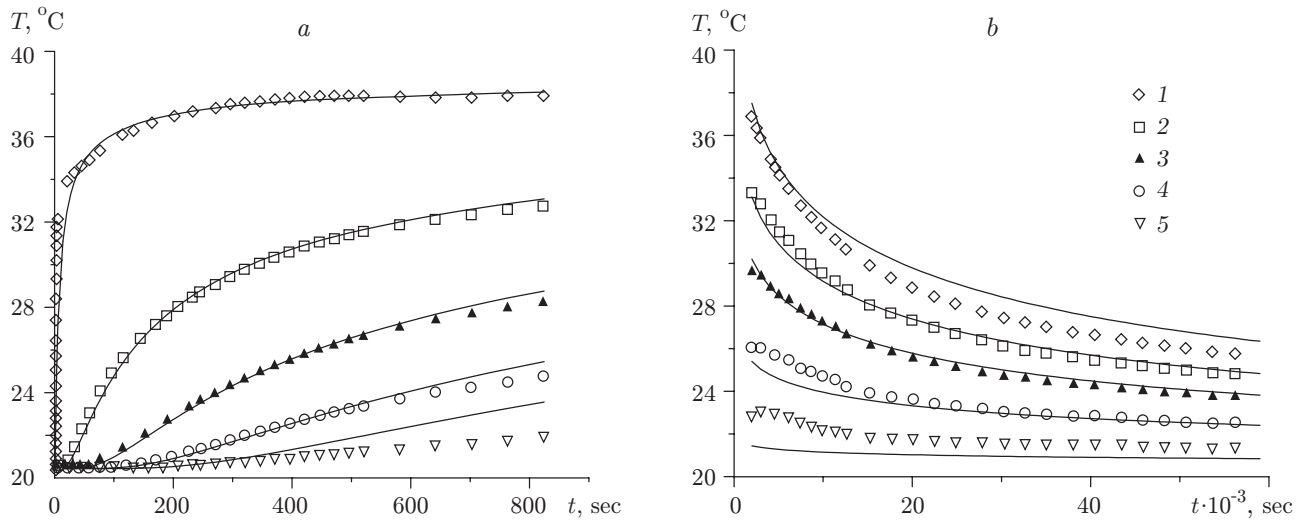


Fig. 4. Temperature versus time at various heights above the bottom at short (a) and long (b) times: $h = 20$ (1), 15 (2), 10 (3), 5 (4), and 0.5 mm (5); the points and curves are the experimental and calculated data, respectively.

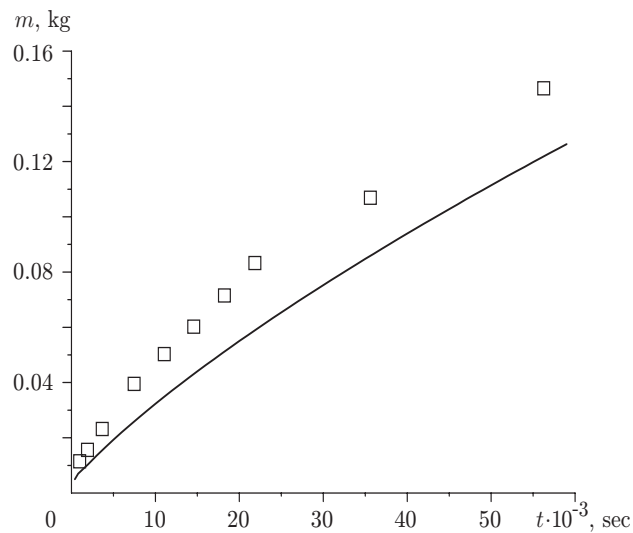


Fig. 5. Absorbed mass versus time: the points and curves are the experimental and calculated data, respectively.

The measured concentration profiles are shown in Fig. 3. Figure 4 shows temperature versus time at various heights above the bottom as compared to the solutions obtained for short and long times [see formulas (4), (6), and (7)]. For short t , we used a quadratic dependence of concentration on temperature to describe the equilibrium state at the interface. A comparison shows that the best agreement between the calculated and experimental data is observed at short t .

The absorbed mass versus time is shown in Fig. 5. The predicted values are 15–20% lower than the measured ones, which can be attributed to imperfectness of the model (especially for long t), to insufficiently high measurement accuracy, or to possible inadequacy of the experimental conditions adopted in the present study to the assumptions laid to the basis of the models.

This work was supported by the Russian Foundation for Fundamental Research (Grant No. 00-15-96177).

REFERENCES

1. V. E. Nakoryakov and N. I. Grigor'eva, "Exact solution of the problem of combined heat and mass transfer during film absorption," *Inzh.-Fiz. Zh.*, **33**, No. 5, 893–896 (1977).
2. V. E. Nakoryakov and N. I. Grigor'eva, "Simulation of heat and mass transfer under nonisothermal absorption on the initial length of downward film flow," *Teor. Osn. Khim. Tekhnol.*, **14**, No. 4, 483–488 (1980).
3. G. Grossman, "Simultaneous heat and mass transfer in film absorption under laminar flow," *Int. J. Heat Mass Transfer*, **26**, No. 3, 357–371 (1983).
4. V. E. Nakoryakov and N. I. Grigor'eva, "Heat and mass transfer during film absorption with variation of the liquid-phase volume," *Teor. Osn. Khim. Tekhnol.*, **29**, No. 3, 242–248 (1995).
5. H. Le Goff, A. Ramadane, and P. Le Goff, "Modelisation des transferts couples de matiere et de chaleur dans l'absorption gaz-liquide en film ruisselant laminaire," *Int. J. Heat Mass Transfer*, **28**, No. 11, 2005–2017 (1985).
6. B. J. C. Van der Wekken, R. H. Wassenaar, and A. Segal, "Finite element method solution of simultaneous two-dimensional heat and mass transfer in laminar film flow," *Wärme- und Stoffübertrag.*, No. 22, 347–354 (1988).
7. A. T. Conlisk, "Analytical solutions for the heat and mass transfer in a falling film absorber," *Chem. Eng. Sci.*, **50**, No. 4, 651–660 (1995).
8. N. Brauner, D. M. Maron, and H. Meyerson, "Coupled heat condensation and mass absorption with comparable concentrations of absorbate and absorbent," *Int. J. Heat Mass Transfer*, **32**, No. 10, 1897–1906 (1989).
9. R. Yang and B. D. Wood, "A numerical modeling of an absorption process on a liquid falling film," *Solar Energ.*, **48**, No. 3, 195–198 (1992).
10. V. E. Nakoryakov, A. P. Burdukov, N. S. Bufetov, et al., "Experimental study of nonisothermal absorption in a falling liquid film," *Teor. Osn. Khim. Tekhnol.*, **14**, No. 5, 755–758 (1980).
11. F. Cosenza and G. C. Vliet, "Absorption in falling water/LiBr films on horizontal tubes," *Trans. of Amer. Soc. Heat. Refrig. Air Cond. Engrs*, **96**, Part. 1 (1990).
12. H. Daiguji, E. Hihara, and T. Saito, "Mechanism of absorption enhancement by surfactant," *Int. J. Heat Mass Transfer*, **40**, No. 8, 1743–1752 (1997).
13. S. H. Chang and H. L. Toor, "Gas absorption accompanied by a large heat effect and volume change of the liquid phase," *AIChE J.*, **10**, No. 3, 398–402 (1964).
14. V. E. Nakoryakov and N. I. Grigorieva, "Vapor absorption stagnant layer of solution," *J. Eng. Thermophys.*, **11**, No. 1, 115–127 (2002).
15. H. Lover, "Thermodynamische und physikalische Eigenschaften der wassrigen Lithiumbromid Lösung," Ph.D. Thesis, Karlsruhe (1960).